Published in final edited form as:
Magn Reson Med. 2012 January ; 67(1): 27–33. doi:10.1002/mrm.23001.

Longitudinal *Inter*- and *Intra*-individual Human Brain Metabolic Quantification Over 3 Years With Proton MR Spectroscopy At 3T

Ivan I. Kirov, **Ilena C. George**, **Nikhil Jayawickrama**, **James S. Babb**, **Nissa N. Perry**, and **Oded Gonen**
Department of Radiology, New York University School of Medicine, New York, NY, USA

Abstract

The longitudinal repeatability of proton MR spectroscopy (^{1}H-MRS) in the healthy human brain at high fields over long periods is not established. Therefore, we assessed the *inter*- and *intra*-subject repeatability of ^{1}H-MRS in an approach suited for diffuse pathologies in ten individuals, at 3T, annually for three years. Spectra from 480 voxels over 360cm^3 (~30%) of the brain, were individually phased, frequency-aligned and summed into one average spectrum. This dramatically increases metabolites' signal-to-noise-ratios while maintaining narrow linewidths that improve quantification precision. The resulting concentrations of the *N*-acetylaspartate, creatine, choline and *myo*-inositol are: 8.9±0.8, 5.9±0.6, 1.4±0.1 and 4.5±0.5 mM (mean±standard-deviation). The *inter*-subject coefficients-of-variation (CVs) are 8.7%, 10.2%, 10.7% and 11.8%; and the longitudinal (*intra*-subject) CVs are lower still: 6.6%, 6.8%, 6.8% and 10%, much better than the 35%, 44%, 55% and 62% *intra*-voxel CVs. The biological and non-biological components of the summed spectra CVs had similar contributions to the overall variance.

Keywords

Brain; MR Spectroscopy; diffuse pathology; repeatability

INTRODUCTION

Proton MR spectroscopy (^{1}H-MRS) adds metabolic specificity to the high morphological sensitivity of clinical (T_1- with and without contrast enhancement and T_2-weighted) MRI, both in research and clinical applications (1). Since human ^{1}H-MRS is still predominantly confined to the brain, a number of neurological conditions have been characterized based on the levels of the *N*-acetyl-aspartate (NAA), creatine (Cr), choline (Cho) and *myo*-inositol (*m*I), the most common surrogate markers for neuronal, membrane, cell energetics and glial abnormalities detectable with *in vivo* ^{1}H-MRS (1).

Monitoring diseases with ^{1}H-MRS, however, requires knowledge of the normal cross-sectional and longitudinal variation of these metabolites. Single-voxel (2) and multi-voxel (3,4) studies report *inter*- and *intra*-individual metabolites' coefficients of variation (CVs) as low as 3% to over 20% at 1.5 T, but only five quantified them at the higher, 3T, clinical field with no follow-up longer than a few months (3–7). In addition, given the diffuse nature of most neurological disorders, the small, 10%, brain coverage of single-voxel or two-dimensional (2D) ^{1}H-MRS may: *(i)* not represent global tissue status; *(ii)* be dominated by

Contact for correspondence and reprint requests: Oded Gonen, PhD, Department of Radiology, New York University School of Medicine, 660 First Avenue, 4th Floor, New York, New York 10016, Telephone/FAX: (212) 263-3532/(212) 263-7541, oded.gonen@nyumc.org.

instrumental noise; *(iii)* be influenced by partial volume; and *(iv)* be confounded by volume-of-interest (VOI) misregistration in serial studies.

To reduce the contribution of repositioning and non-biological variation, we summed the phased and frequency-aligned spectra from all 480 voxels of a 3D ^{1}H-MRS acquisition over ~30% of the human brain. Absent a specific hypothesis, whole-VOI summation yields an average spectrum that is relevant to diffuse disorders, yet with the substantial signal-to-noise-ratio (SNR) improvement that is essential for repeatability (8), at minimal cost in spectral resolution. Our two goals, consequently, are to establish the normal brain's cross-sectional and longitudinal (*inter*- and *intra*-subject) NAA, Cr, Cho and *m*I variations. Towards this end we applied annual test-retest brain 3D ^{1}H-MRS in ten healthy subjects over three years at 3T.

MATERIALS AND METHODS

Human Subjects

Ten healthy volunteers (7 women, 3 men) 24 to 43 (mean 30) years old were enrolled. Their "healthy" status was based on self-reported negative answers to a list of disqualifying neurological conditions before the scan and an "unremarkable" MRI subsequently. All gave Institutional Review Board-approved written informed consent.

MR Acquisition

All experiments were done in a 3T Trio whole-body scanner (Siemens AG, Erlangen Germany) with a TEM3000 transmit-receive head-coil (MRInstruments, Minneapolis, MN). Sagittal T1-weighted Magnetization-Prepared RApid Gradient-Echo (MP-RAGE): TE/TI/TR=2.6/800/1360 ms, 256×256 matrix, 256×256 mm^2 field-of-view (FOV), 160 slices, 1 mm thick MRI were obtained from each subject for VOI-guidance and tissue segmentation.

Our chemical-shift-imaging (CSI) based automatic procedure adjusted the scanner's first and second order shims in 3–5 minutes. A 10 cm anterior-posterior (AP) ×8 cm left-right (LR) ×4.5 cm inferior-superior (IS) =360 cm^3 VOI was centered over the corpus callosum and aligned along its genu–splenium line, as shown in Fig. 1. The VOI was excited using PRESS (*TE/TR*= 35/1800 ms) with three second-order Hadamard encoded slabs (6 slices) sequentially multiplexed along the IS direction every *TR*, for optimal SNR and spatial coverage (9). Its strong, 6 mT/m, Hadamard slice select gradient reduced the chemical shift displacement between NAA and *m*I to ~0.6 mm, 8% of the slice width. The slices' planes were encoded with 16×16 2D-CSI over a 16×16 cm^2 (LR×AP) FOV. The VOI was defined in their planes by two 11.2 ms long 180° pulses under 1.35 mT/m in the LR and 1.1 mT/m in the AP directions, resulting in 0.35 and 0.44 cm chemical shift displacement in the LR and AP directions only at VOI edges. The MR signal was acquired for 256ms at ±1 kHz bandwidth. Each 16×16×6 ^{1}H-MRS measurement took 15 minutes and with two averages the protocol was under an hour.

VOI volumetry

Since the VOI also includes lateral ventricles and sulci (*cf.* Fig. 1), correction for their cerebro-spinal fluid (CSF) partial volume is needed. To determine total tissue, white and gray matter (WM, GM) VOI fractions (T_f, WM_f, GM_f), the MP-RAGE images were segmented using SPM2 (10). In-house software then calculated the WM, GM and CSF volume inside the VOI and converted them into T_f, WM_f, GM_f by dividing by the 360 cm^3 VOI volume.

^{1}H-MRS-metabolite quantification

The ^{1}H-MRS data was voxel shifted to align the CSI grid with the NAA VOI, Fourier transformed in the time, AP and LR dimensions and Hadamard reconstructed along the IS direction using in-house software. The 480 VOI's spectra were each frequency-aligned and zero-order phased in reference to the NAA peak, then summed. This retained the (narrow) linewidth of the individual spectra *and* improved the SNR by a factor of ~$480^{½}$, as shown in Fig. 2.

Relative levels of the i^{th} (i=NAA, Cr, Cho, *m*I) metabolite in the j^{th} (j=1..10) subject were estimated from their peak area, S_{ij}, using the SITools-FITT spectral modeling software (11). The S_{ij} were then scaled into absolute concentration, C_{ij}, relative to a 2 L sphere of C_i^{vitro}=12.5, 10.0, 3.0 and 7.5 mM NAA, Cr, Cho and *m*I in water at physiological ionic strength to load the coil:

$$C_{ij}=C_i^{vitro}\cdot\frac{S_{ij}}{S_R}\cdot\frac{V_j^{180^\circ}}{V_R^{180^\circ}}\cdot\frac{1}{\mathrm{T_f}}, \quad [1]$$

where S_R is the sphere's metabolites' signal, $V_j^{180^\circ}$ and $V_R^{180^\circ}$ are the RF voltages needed for a non-selective 1 ms 180° inversion pulse on subject and reference sphere. The C_{ij}s were corrected for relaxation time differences *in vivo* (T_1^{vivo}, T_2^{vivo}) and *in vitro* (T_1^{vitro}, T_2^{vitro}) with a factor (12):

$$f=\frac{\exp(-TE/T_2^{vitro})}{\exp(-TE/T_2^{vivo})}\cdot\frac{1-\exp(-TR/T_1^{vitro})}{1-\exp(-TR/T_1^{vivo})}. \quad [2]$$

Since the composition of the VOI is about 60:40% WM:GM (Table 1), weighted averages: T_2^{vivo}=350, 174, 251 and 200 ms for NAA, Cr, Cho and *m*I (13,14); and T_1^{vivo}=1360, 1300, 1145 and 1024 ms at 3T were used (14,15). The respective values in the phantom were T_2^{vitro}=483, 288, 200, 233 ms and T_1^{vitro}=605, 366, 235, 280 ms.

Strategy

To determine the non-biological component of the variances and to increase the metabolites' SNRs, two back-to-back 16×16×4 ^{1}H-MRS measurements were acquired at each session (without changing the position or acqusition parameters). These two should exhibit only minor differences due to electronic noise and patient motion, but not from biological variation. To establish the *inter*-subject variance, 10 volunteers were scanned as described above. The variance between these sessions comprising *inter*-subject biological variations, all the "non-biological" components enumerated above, plus any differences in reposition or shim. To determine the *intra*-subject variance, each of ten was scanned three additional times annually with the VOI repositioned as close to its original location as the MRI allowed the operator. The variance between these sessions comprises the sum of the *intra*-subject biological variations and all the non-biological components.

Statistical Analysis

The 40 back-to-back measurements yielded 80 (10 subjects ×4 sessions each ×2 measurements/session) data-sets. The biological and non-biological components of the *intra*- and *inter*-subject variances of the sums were assessed using restricted maximum

likelihood (REML) estimation of variance components within a random effects model. Specifically, REML was used to estimate the variation between measures derived for each metabolite: *(i)* at the same time for the same subject on the 80 data sets; *(ii)* at different times for the same subject on the 40 data sets (10 subjects ×4 sessions each), aka the *intra*-subject variation; and *(iii)* between (*inter*-)subjects variation. The overall variance was estimated for each metabolite as the variance among the 80 measurements included in the analysis.

To calculate the repeatability of the sums we used 40 (10 subjects ×4 sessions each) scans, each comprising two measurements. The *inter*- and *intra*-subject CVs of the sums for each metabolite were estimated by dividing the standard deviation (SD) of the between- and within-subject variance by the overall mean (over subjects and time points). To compare the repeatability of these with that of the single, 0.75 cm^3 voxels, *intra*-voxel CVs were calculated from the two back-to-back measurements: the SD of the within-voxel concentration differences of all 480 spectra was divided by the overall mean of that subject. Values over 2.5 SDs from the overall mean were excluded from the analysis (~2% of all voxels).

Finally, we conducted temporal and cross-sectional sensitivity analyses on the sums. The sample size needed to detect a metabolite's group mean rate of change with 80% power was calculated under the assumptions that each subject will provide 4 annual time points. The true group mean annual rate of change was assumed to correspond to an annual change of either 5%, 10% or 15% of the baseline mean. Sensitivity to observe metabolic and volumetric changes between two scans was estimated according to (16):

$$\text{Sensitivity}=2\sqrt{2}\times \text{SD}/\sqrt{N}, \quad [3]$$

for N subjects. That is, sensitivity is defined as the precision for estimating the mean difference for an individual or a group with a 95% confidence interval assuming a known variance (16).

RESULTS

Our automated shim procedure yielded consistent 27±5 Hz (mean±standard deviation) full width at half-maximum (FWHM) whole-head water line, improving to 22±3 Hz in the VOI without additional adjustments. An example of the VOI size, position and spectra, is shown in Fig. 1. The average NAA, Cr, Cho and *m*I SNRs, estimated as peak-height divided by twice the root-mean-square noise in 19,200 voxels (10 subjects ×480 spectra each ×4 times) were: 30±6, 15±3, 13±2 and 8±1. The metabolites' FWHM linewidth was 5.4±1.3 Hz, *i.e.*, T_2^* ($1/\pi\Delta\omega$ assuming Lorentzian lines) of 59±12 ms.

The SNR and linewidth gains of alignment and summation are demonstrated by comparing a single voxel spectrum with an aligned and a non-aligned sums in Fig. 2. The latter, equivalent to a whole-VOI PRESS, suffers a clear 2.5 fold broader lines from global $\mathbf{B_0}$ inhomogeneities (17). Since small voxels suffer less from this effect (17), pre-alignment preserves their narrow lines (compare Figs. 2a with 2c). The aligned sums of 480 VOI spectra for all 10 subjects and time points, overlaid with their model functions, are shown in Fig. 3. They exhibit NAA, Cr, Cho and *m*I SNRs of: 561±74, 265±34, 228±32 and 128±17, a dramatic $\sim 480^{1/2} \approx 22$ gain compared with the 0.75 cm^3 voxels in the source ^{1}H-MRS (compare Fig. 3 with Fig. 1).

Average absolute NAA, Cr, Cho and *m*I concentrations at each time point are compiled in Table 1 and grand averages shown in Table 2. The *inter*- and *intra*-subject SDs and CVs are

compiled in Table 2 and their distributions shown in Fig. 4 along with the *intra*-voxels' distributions for comparison. The results show that the *inter*-subject NAA, Cr, Cho and *m*I CVs: 8.7%, 10.2%, 10.7% and 11.8% are (as expected) higher than the *intra*-subjects': 6.6%, 6.8%, 6.8% and 10%. Although similar CVs are obtained if all voxels in the VOI are first fitted individually and results are then averaged, this process is 480 times longer (several hours) and does not provide easy visualization of results due to the large number of spectra and much lower SNRs. The much higher respective *intra*-voxel (35%, 44%, 55% and 62%) CVs reflect the improved repeatability of the VOI sums, a consequence of their better SNR (8).

The values for WM_f, GM_f and T_f in the VOI are compiled in Tables 1 and 2 and their distributions shown in Fig. 4. Their *inter*-subject CVs: 4.8%, 6.1% and 1.8%, were also higher than the *intra*-subject: 1.2%, 1.6% and 0.7%. This most likely reflects the minimal partial tissue volume variations in serial (large) VOI placement.

Based on the metabolic CVs, to design a study that will have 80% power to detect 5%, 10% or 15% mean annual rates of change would require: 23, 8 and 6 subjects for NAA; 29, 9 and 7 for Cr; 32, 10 and 8 for Cho; 43, 13, and 9 for *m*I. Sensitivities to changes between two scans of a single individual and between two groups of 20 subjects are, respectively: 20% and 4% for NAA, Cr and Cho, and 30% and 7% for mI.

Finally, both the *inter*- and *intra*-subject CVs combine biological and non-biological components. The contribution of the latter to the observed variance can be estimated since each of the 40 sessions comprises two back-to-back measurements that differ only minimally due to electronic noise and possible patient motion. The 80 observations show that the overall variances for NAA, Cr, Cho and *m*I have non-biological contributions of 68%, 55%, 35% and 57%. The *intra*-subject biological contributions were 12%, 2%, 39% and 11%, and the respective *inter*-subjects': 21%, 43%, 28% and 33%.

DISCUSSION

Due to minimal motion, absence of contaminating lipid signals and easier shimming, most applications of ^{1}H-MRS are in the brain. ^{1}H-MRS detected metabolites serve as surrogate markers for various disease processes, providing extra specificity to basic research and clinical protocols for a range of neurological disorders (1). Nevertheless, although other MR metrics are used as surrogates for efficacy in clinical trials, ^{1}H-MRS has not been employed as a primary or even secondary outcome measure in large-scale treatment outcome studies (18). This may be because in order to be considered a method must be *(a)* reproducible, *(b)* clinically relevant, *(c)* pathologically specific; and *(d)* sensitive to changes over time (19). While *(b)* and *(c)* are already established for ^{1}H-MRS, our goal was to address *(a)* and *(d)* for diffuse diseases.

Our approach of synthesizing one spectrum from the sum of all phased and aligned spectra in the VOI enabled us to address both the repeatability and precision issues. Specifically, it yields much higher (×20 fold) metabolite SNRs and consequently lower CVs (8) by exploiting *(i)* the $\mathbf{B_0}$ homogeneity (narrow linewidth) across the individual small voxels (17); and *(ii)* post-acquisition correction for regional $\mathbf{B_0}$ variations (frequency shifts). In addition, summation also averages out chemical shift displacement errors, reducing this effect that can be substantial in individual VOI edge-voxels. These advantages are reflected in Fig. 4, where the *intra*-subject variations are ×4-×5 fold smaller than the 0.75 cm^3 *intra*-voxel ones. Operationally, this means that single voxels of that size would not be sensitive to changes on the order of 9%-24% reported for example in multiple sclerosis (20), whereas the proposed approach has the power to do so in one measurement.

The two 15 minute measurements in every session were obtained back-to-back, *i.e.*, with identical VOI position and shimming (although not accounting for possible motion either within or between each). It is noteworthy, however, that such motions are always encountered by all 3D MRS procedures of this length and that their cumulative effects are included in the overall variation. The back-to-back approach allowed us to assign the variations between these two measurements (the *intra*-voxel differences) exclusively to non-biological contributions.

The order-of-magnitude higher spatial coverage of the sum: 360 versus 3–20 cm^3 for single-voxel methods (21), also minimizes GM/WM/CSF partial volume variations in serial studies, as reflected by the narrow *inter*- and *intra*-subject WM_f, GM_f and T_f distributions depicted in Fig. 4 and their small CVs compiled in Table 2.

The ‹ 12% *inter*-subject CVs of the sums in Table 2 indicate “good” [relative to metabolic changes in neurological disorders (1,22)] cross-sectional similarity between healthy subjects. The longitudinal *intra*-subject repeatability is even better, with 27% lower CVs. These results fall in the “lower” (better) range of the 8%–29% reported for *inter*-subject and 3%–26% CVs for *intra*-subject in single-voxels (2,5,16,22) studies or the 3%–30% *inter*-subject and 5%–27% *intra*-subject CVs reported in multi-voxel studies (23,24). It is also noteworthy that while none of the previous serial studies extended for more than a few months, the data presented here span four points over three years.

The results reveal that the “non-biological” component of the variance of the sums (obtained by comparing two back-to-back scans), is about half of the total variance. Although more averages (or bigger VOI) could, therefore, at least theoretically reduce the former by improving the SNR (8), it cannot reduce the total variance below the true *inter*- and *intra*-subject biological variations. More averaging to increase precision, therefore, may quickly reach diminishing returns considering the time required, and the fact that there is little room for improvement on these CVs that are already at or below 10% and likely cannot be brought down below ~5%.

Knowledge of the CVs can also be used to (*i*) power studies correctly and to weigh (based on cost and recruitment potential) the numbers of subjects versus scans per subject; and (*ii*) discern pathogenesis (or treatment) effects from experimental fluctuations. Specifically, sample sizes of between 7 and 43 subjects are needed for establishing statistical significance for 5%, 10% or 15% rate of annual change with 4 annual data points. Furthermore, differences larger than 20% for NAA, Cr and Cho or 30% for *m*I between two successive scans on one individual would be significant. These drop substantially, to just 4% and 7% respectively, for 20 subjects.

The main limitation of the proposed approach is that the gains in repeatability come at the cost of all focal or even regional metabolic information. This tradeoff may be acceptable, however, in studies of diffuse disorders where sensitivity to global changes may outweigh the need for localized information. Note, however, that hypotheses that require regional or tissue-specific sampling can still be tested since the original localized data is available.

Acknowledgments

This work was supported by NIH Grants NS050520, NS39135, NS29029 and EB01015.

References

1. Mountford CE, Stanwell P, Lin A, Ramadan S, Ross B. Neurospectroscopy: the past, present and future. Chem Rev. 2010; 110(5):3060–3086. [PubMed: 20387805]

2. Traber F, Block W, Freymann N, Gur O, Kucinski T, Hammen T, Ende G, Pilatus U, Hampel H, Schild HH, Heun R, Jessen F. A multicenter reproducibility study of single-voxel 1H-MRS of the medial temporal lobe. Eur Radiol. 2006; 16(5):1096–1103. [PubMed: 16416279]

3. Maudsley AA, Domenig C, Sheriff S. Reproducibility of serial whole-brain MR spectroscopic imaging. NMR Biomed. 2010; 23(3):251–256. [PubMed: 19777506]

4. Gasparovic C, Bedrick EJ, Mayer AR, Yeo RA, Chen H, Damaraju E, Calhoun VD, Jung RE. Test-retest reliability and reproducibility of short-echo-time spectroscopic imaging of human brain at 3T. Magn Reson Med. 2011

5. Hancu I, Blezek DJ, Dumoulin MC. Automatic repositioning of single voxels in longitudinal 1H MRS studies. NMR Biomed. 2005; 18(6):352–361. [PubMed: 15954181]

6. Wellard RM, Briellmann RS, Jennings C, Jackson GD. Physiologic variability of single-voxel proton MR spectroscopic measurements at 3T. AJNR Am J Neuroradiol. 2005; 26(3):585–590. [PubMed: 15760870]

7. Wijnen JP, van Asten JJ, Klomp DW, Sjobakk TE, Gribbestad IS, Scheenen TW, Heerschap A. Short echo time 1H MRSI of the human brain at 3T with adiabatic slice-selective refocusing pulses; reproducibility and variance in a dual center setting. J Magn Reson Imaging. 2010; 31(1):61–70. [PubMed: 20027568]

8. Kreis R, Slotboom J, Hofmann L, Boesch C. Integrated data acquisition and processing to determine metabolite contents, relaxation times, and macromolecule baseline in single examinations of individual subjects. Magn Reson Med. 2005; 54(4):761–768. [PubMed: 16161114]

9. Goelman G, Liu S, Hess D, Gonen O. Optimizing the efficiency of high-field multivoxel spectroscopic imaging by multiplexing in space and time. Magn Reson Med. 2006; 56(1):34–40. [PubMed: 16767711]

10. Ashburner J, Friston KJ. Voxel-based morphometry--the methods. Neuroimage. 2000; 11(6 Pt 1): 805–821. [PubMed: 10860804]

11. Soher BJ, Young K, Govindaraju V, Maudsley AA. Automated spectral analysis III: application to in vivo proton MR spectroscopy and spectroscopic imaging. Magn Reson Med. 1998; 40(6):822–831. [PubMed: 9840826]

12. Inglese M, Li BS, Rusinek H, Babb JS, Grossman RI, Gonen O. Diffusely elevated cerebral choline and creatine in relapsing-remitting multiple sclerosis. Magn Reson Med. 2003; 50(1):190–195. [PubMed: 12815694]

13. Kirov I, Fleysher L, Fleysher R, Patil V, Liu S, Gonen O. Age dependence of regional proton metabolites T2 relaxation times in the human brain at 3 T. Magn Reson Med. 2008; 60(4):790–795. [PubMed: 18816831]

14. Posse S, Otazo R, Caprihan A, Bustillo J, Chen H, Henry PG, Marjanska M, Gasparovic C, Zuo C, Magnotta V, Mueller B, Mullins P, Renshaw P, Ugurbil K, Lim KO, Alger JR. Proton echo-planar spectroscopic imaging of J-coupled resonances in human brain at 3 and 4 Tesla. Magn Reson Med. 2007

15. Traber F, Block W, Lamerichs R, Gieseke J, Schild HH. 1H metabolite relaxation times at 3.0 tesla: Measurements of T1 and T2 values in normal brain and determination of regional differences in transverse relaxation. J Magn Reson Imaging. 2004; 19(5):537–545. [PubMed: 15112302]

16. Brooks WM, Friedman SD, Stidley CA. Reproducibility of 1H-MRS in vivo. Magn Reson Med. 1999; 41(1):193–197. [PubMed: 10025629]

17. Li BS, Regal J, Gonen O. SNR versus resolution in 3D 1H MRS of the human brain at high magnetic fields. Magn Reson Med. 2001; 46(6):1049–1053. [PubMed: 11746567]

18. De Stefano N, Filippi M, Miller D, Pouwels PJ, Rovira A, Gass A, Enzinger C, Matthews PM, Arnold DL. Guidelines for using proton MR spectroscopy in multicenter clinical MS studies. Neurology. 2007; 69(20):1942–1952. [PubMed: 17998486]

19. Miller DH. Biomarkers and surrogate outcomes in neurodegenerative disease: lessons from multiple sclerosis. NeuroRx. 2004; 1(2):284–294. [PubMed: 15717029]

20. Kirov I, Patil V, Babb JS, Rusinek H, Herbert J, Gonen O. MR spectroscopy indicates diffuse multiple sclerosis activity during remission. J Neurol Neurosurg Psychiatry. 2009; 80(12):1330–1336. [PubMed: 19546105]

21. Barker, P. Fundamentals of MR Spectroscopy. Barker, P., editor. Cambridge: Cambridge University Press; 2005. p. 7-27.

22. Rosen Y, Lenkinski RE. Recent advances in magnetic resonance neurospectroscopy. Neurotherapeutics. 2007; 4(3):330–345. [PubMed: 17599700]

23. Chard DT, McLean MA, Parker GJ, MacManus DG, Miller DH. Reproducibility of in vivo metabolite quantification with proton magnetic resonance spectroscopic imaging. J Magn Reson Imaging. 2002; 15(2):219–225. [PubMed: 11836781]

24. Li BS, Babb JS, Soher BJ, Maudsley AA, Gonen O. Reproducibility of 3D proton spectroscopy in the human brain. Magn Reson Med. 2002; 47(3):439–446. [PubMed: 11870829]

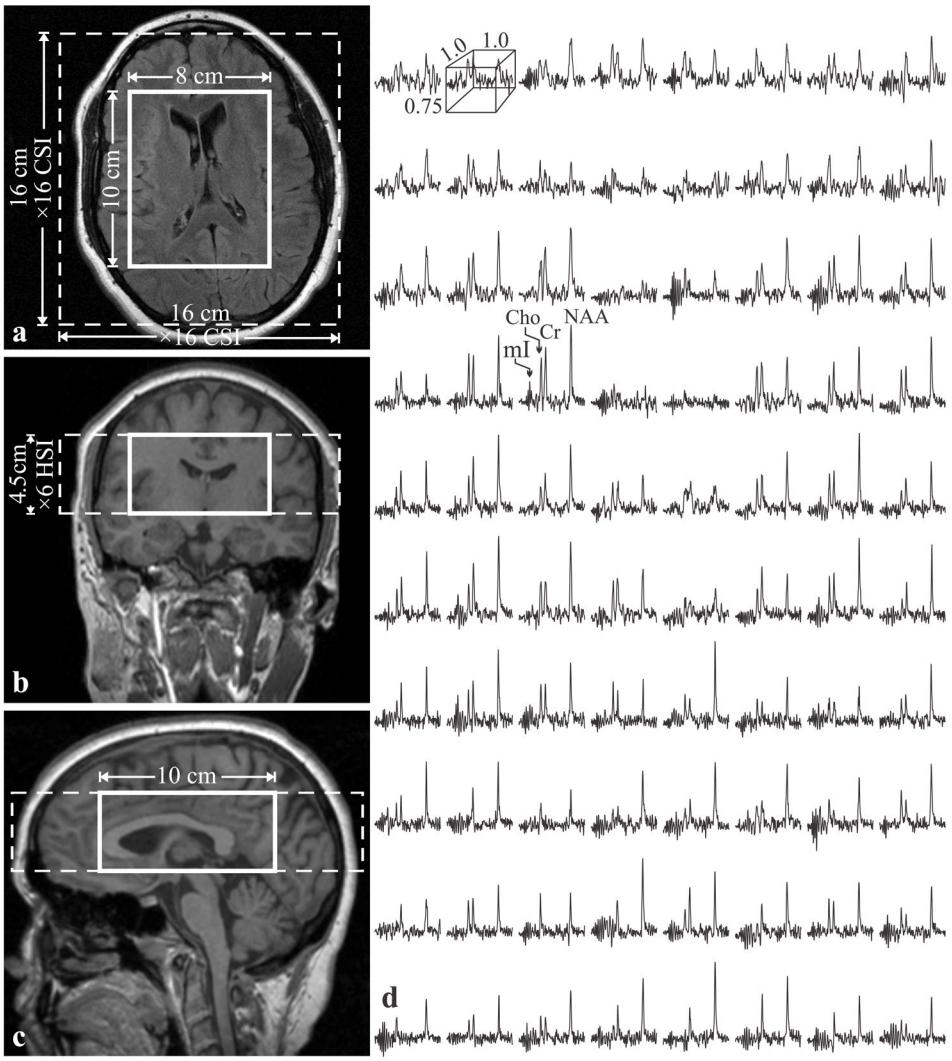

Fig. 1.

Left: Axial (**a**), coronal (**b**) and sagittal (**c**) MRI superimposed with the 3D ^{1}H-MRS FOV and VOI (dashed and solid white frames). Right: Real part of the 8×10 (LR×AP) ^{1}H spectra matrix from the VOI on **a**, on common frequency (1.4 to 3.8 ppm) and intensity scales. Note the spectral resolution and SNR in these 0.75 cm^{3} voxels obtained in 30 minutes of acquisition.

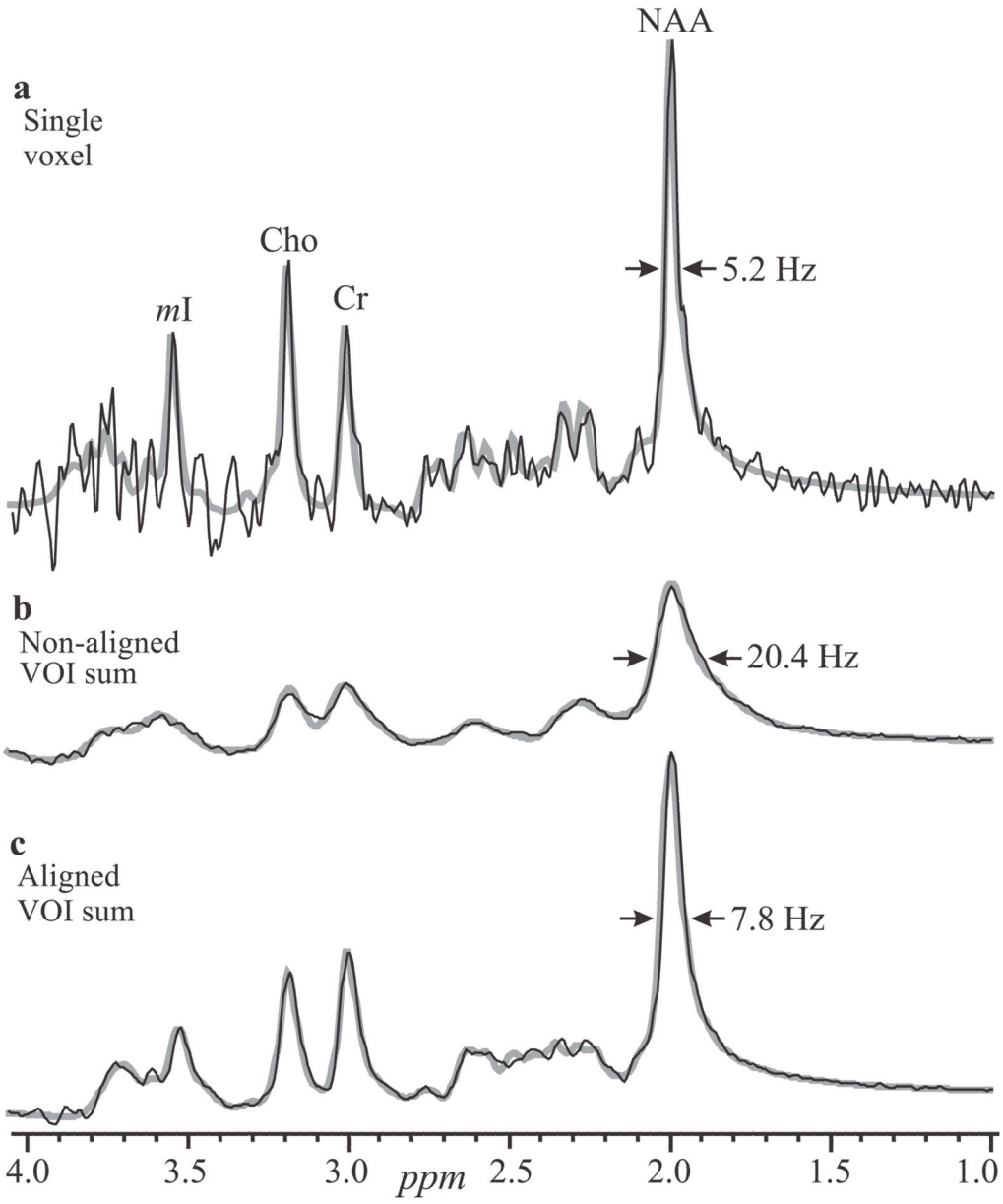

Fig. 2.

Real part of ^{1}H spectra (black lines) superimposed with their fitted model functions (gray lines). Top, **a**: Spectrum from a single 0.75 cm^3 voxel from subject #8 in Table 1. **b**: Non-aligned sum of all 480 spectra in the VOI (equivalent to a 360 cm^3 single-voxel acquisition) of the same subject. Note the better SNR compared with **a**, but ×2.5 fold degraded linewidth. Bottom, **c**: Same as **b**, but with spectral alignment prior to summation, resulting in ×2.5 better spectral resolution *and* SNR compared with **b**.

Fig. 3.

Real part of the 480 pre-aligned then summed ^{1}H spectra from the VOI of each of the 10 subjects *and* their 4 annual time point (black lines) superimposed with the fitted model functions (gray lines) on common frequency and intensity scales. Note: *(i)* the excellent 130 (*m*I) – 560 (NAA) SNRs and linewidths of the sums compared with the individual voxels in Fig. 1; *(ii)* the quality of the fit; and *(iii)* the visual similarity in metabolic levels both among the subjects (*inter*-individual) at each time point, and between time points (*intra*-individual).

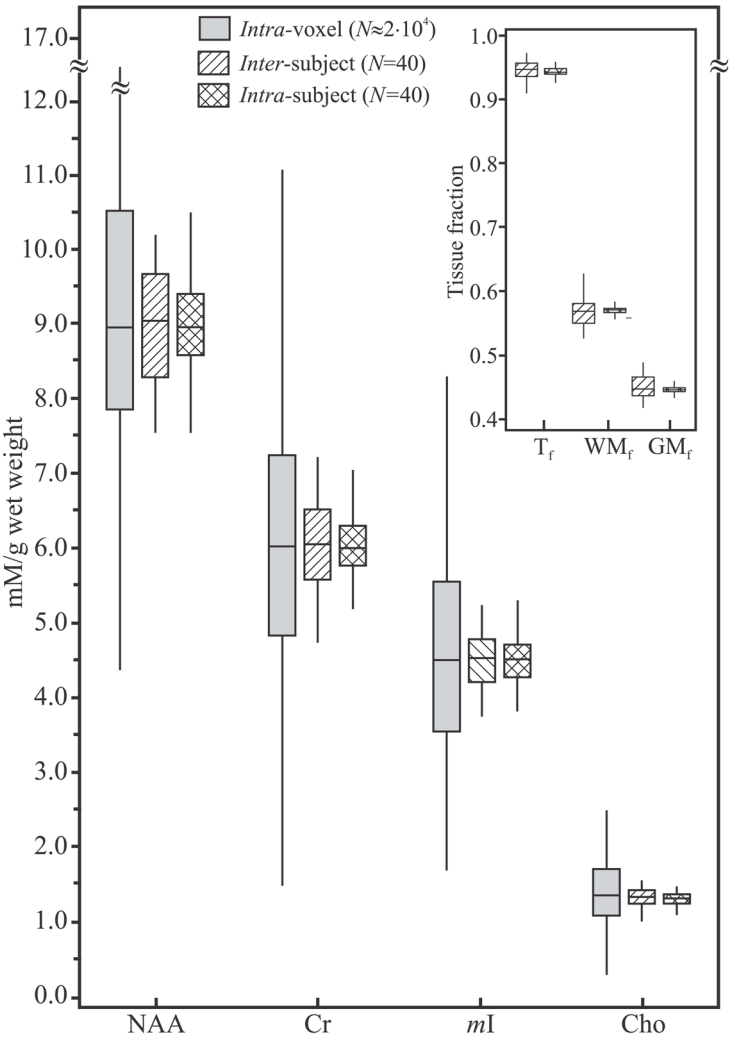

Fig. 4.

Box plots displaying the 25th, median and 75th (box) as well as ±95th percentiles (whiskers) of the NAA, Cr, Cho and *m*I absolute concentrations distributions for single voxels, *intra*-voxel, shaded; and the summed spectra: single time points across all subjects (*inter*-subject, right-hatched) and all time points of the same subject (*intra*-subject, cross-hatched). Note the dramatic, ×4 to ×5 fold, improvement in both cross-sectional and longitudinal repeatability of the sums compared with the single voxels. Insert: Box plots of the GM, WM and tissue fractions (GM_f, WM_f and T_f) distributions in the VOIs of all subjects. Note the narrow distribution of tissue types, indicating the minimal GM/WM/CSF partial volume repositioning error of the proposed approach.

Table 1

Mean±standard deviation of the volumetric (MRI) and metabolic (^{1}H-MRS) data for all subjects at each scanning interval.

				^{1}H-MRS (mM)			
[a] Scanning interval	WM fraction	[b] MRI GM fraction	Tissue fraction	NAA	Cr	Cho	*m*I
0	0.57±0.03	0.43±0.03	0.95±0.02	8.8±0.7	5.8±0.5	1.3±0.1	4.5±0.5
12	0.57±0.03	0.43±0.03	0.95±0.01	8.9±0.6	5.8±0.5	1.4±0.1	4.4±0.8
25	0.56±0.03	0.44±0.03	0.95±0.02	9.2±1	6.1±0.8	1.4±0.2	4.6±0.5
36	0.56±0.03	0.44±0.03	0.95±0.02	8.8±0.9	5.9±0.7	1.3±0.1	4.5±0.4

[a] Months,

[b] inside the VOI.

Table 2

The estimated standard deviations (SD) and coefficients of variation (CVs) (parenthesis) between (*inter*-) and within (*intra*-) subjects' metabolic concentrations (mM) and tissue fractions. The rightmost column represents the average±SD of each metric over the 40 measurements (10 subjects ×4 data points) and the overall CVs (%).

		***Inter*-subject**	***Intra*-subject**	**Metric±SD (CV)**
MRS (mM)	NAA	0.8 (8.7%)	0.6 (6.6%)	8.9±0.8 (8.9%)
	Cr	0.6 (10.2%)	0.4 (6.8%)	5.9±0.6 (10.5%)
	Cho	0.1 (10.7%)	0.1 (6.8%)	1.4±0.1 (11%)
	*m*I	0.5 (11.8%)	0.5 (10%)	4.5±0.5 (11.9%)
MRI	WM_f	0.03 (4.8%)	0.01 (1.2%)	0.57±0.03 (4.8%)
	GM_f	0.03 (6.1%)	0.01 (1.6%)	0.44±0.03 (6.1%)
	T_f	0.02 (1.8%)	0.01 (0.7%)	0.95±0.02 (1.8%)